

Supporting Information

Hierarchical Nanoporous V₂O₃ Nanosheets Anchored with Alloy Nanoparticles for Efficient Electrocatalysis

Haitao Xu,^a Li Liu,^c Jiaojiao Gao,^b Peng Du,^b Gang Fang,^b Hua-Jun Qiu^{b*}

^a School of Materials Science and Engineering, Dongguan University of Technology, Dongguan 523808, China

^b School of Materials Science and Engineering, Harbin Institute of Technology, Shenzhen 518055, China

^c Chongqing Key Laboratory of Green Synthesis and Applications, College of Chemistry, Chongqing Normal University, Chongqing City 401331, China

*E-mail: qiuahuajun@hit.edu.cn

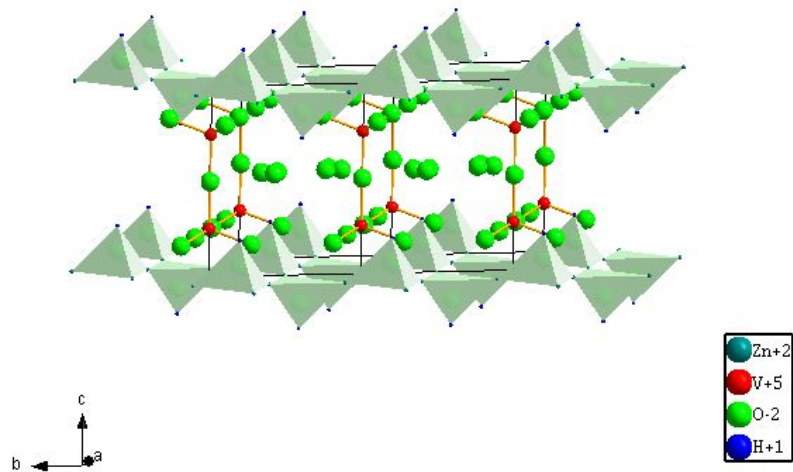


Figure S1 Crystal structure of the VZn-LDHs.

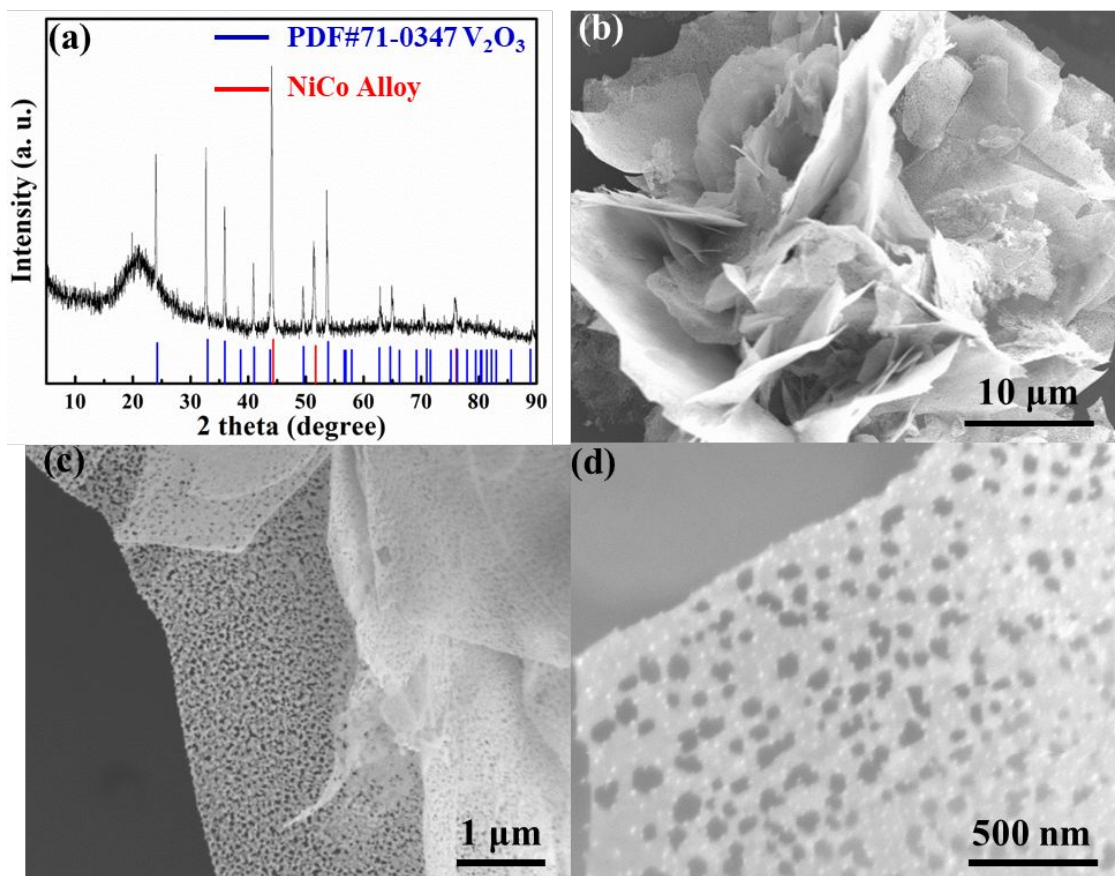


Figure S2 (a) XRD patterns of the $\text{NiCo}@\text{V}_2\text{O}_3$; (b), (c), and (d) SEM images of $\text{NiCo}@\text{V}_2\text{O}_3$ nanosheets with different magnification.

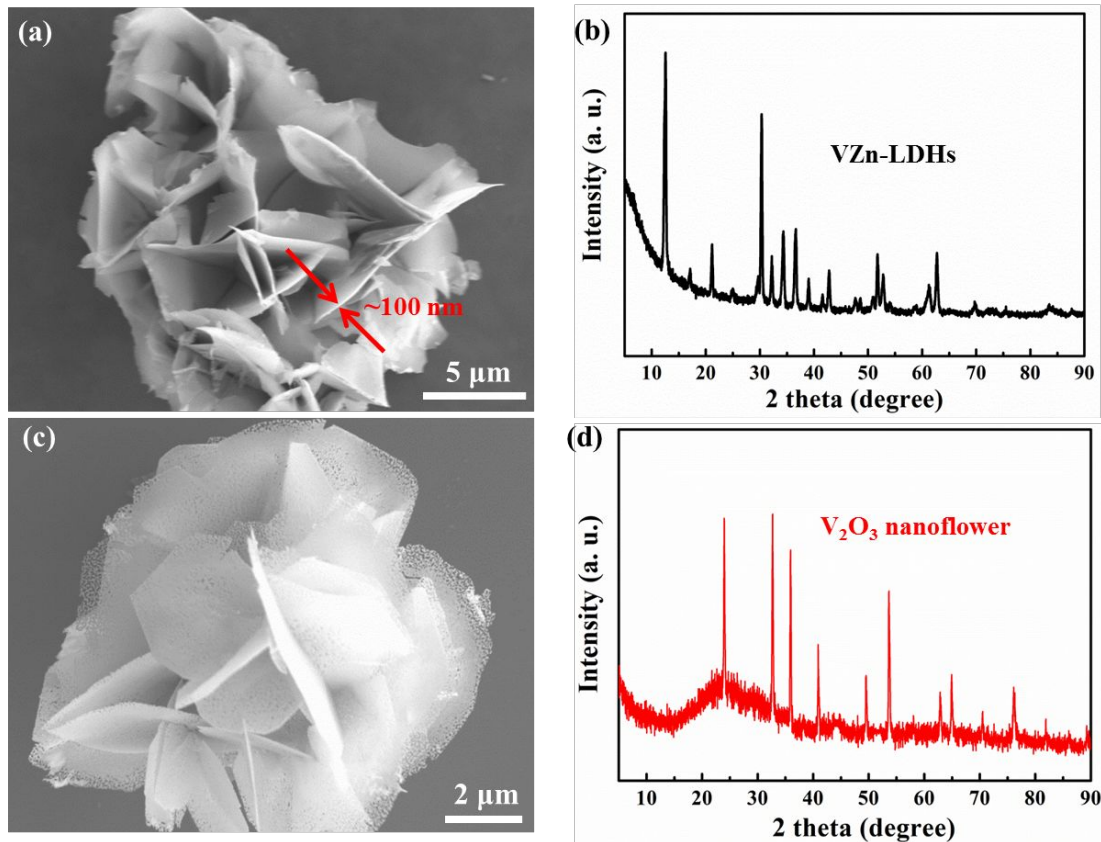


Figure S3 (a) SEM image of VZn-LDHs; (b) XRD patterns of the VZn-LDHs; (c) SEM image of V_2O_3 nanosheets; (d) XRD pattern of the V_2O_3 sheets.

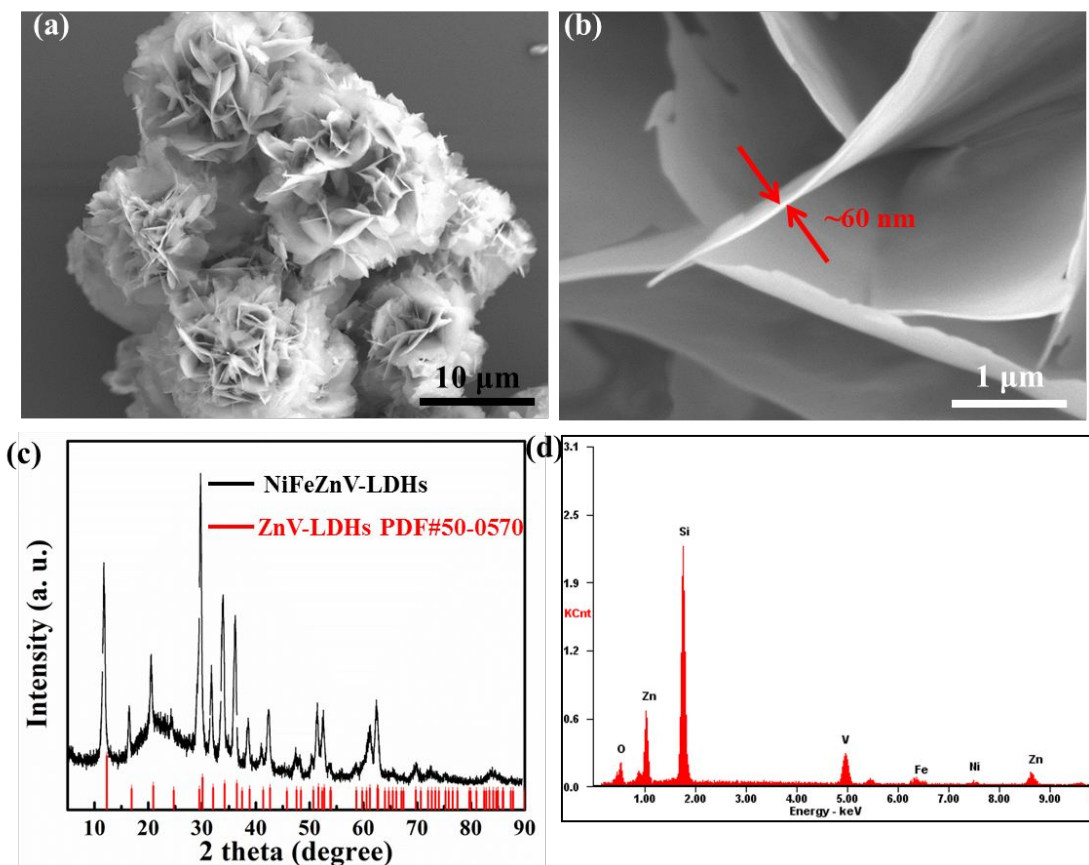


Figure S4 Low- (a) and high-magnification (b) SEM images of NiFeZnV-LDHs precursor; XRD pattern (c) and EDS line profile (d) of the NiFeZnV-LDHs precursor.

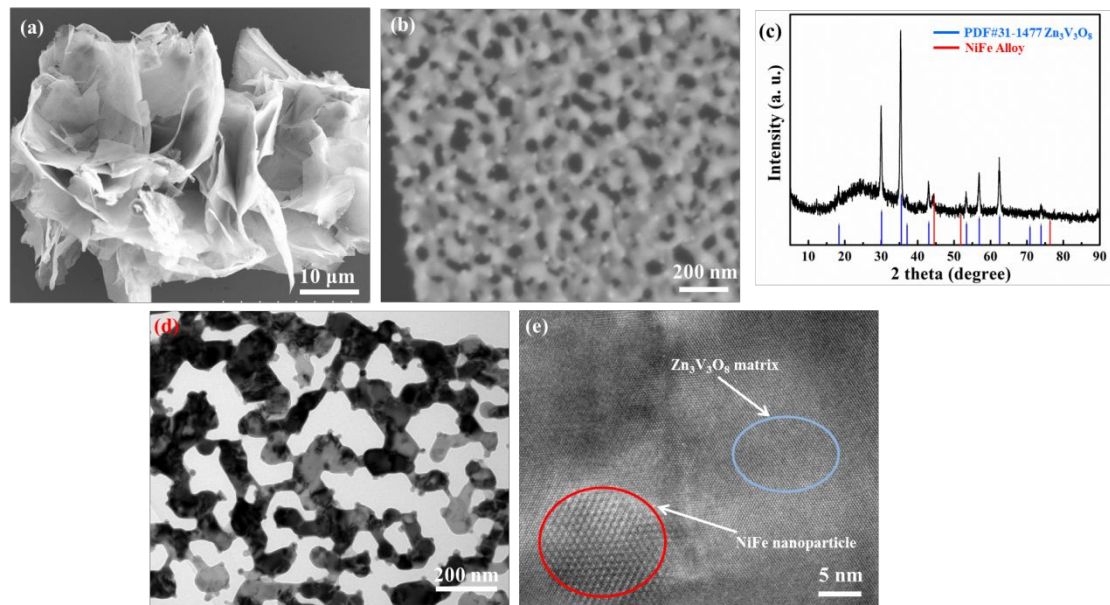


Figure S5 Low- (a) and high-magnification (b) SEM images of NiFe@Zn₃V₃O₈; XRD patterns (c), TEM image (d), and HRTEM (e) image of NiFe@Zn₃V₃O₈.

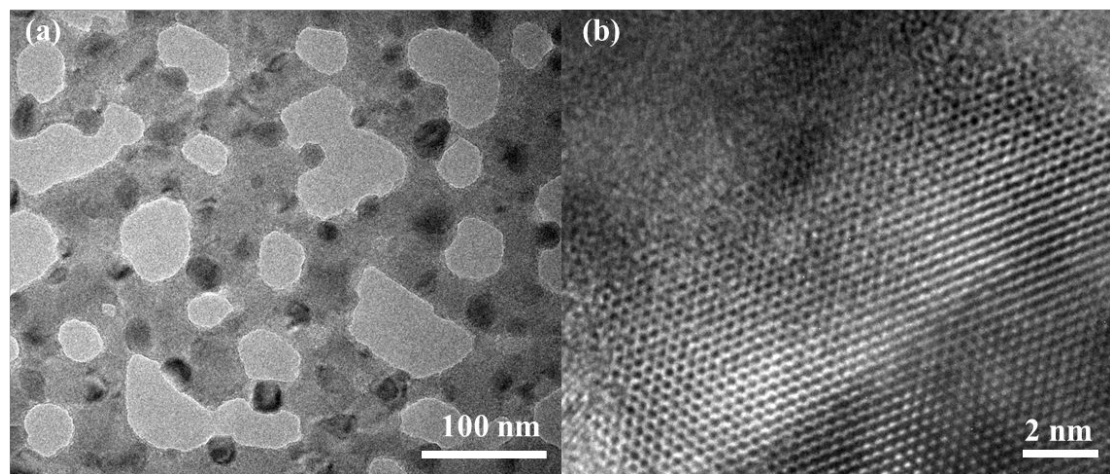


Figure S6TEM image of NiFe@V₂O₃ hybrid (a), and the HRTEM image (b) focused at the edge of the NiFe nanoparticle to discover the crystal defects and lattice distortions.

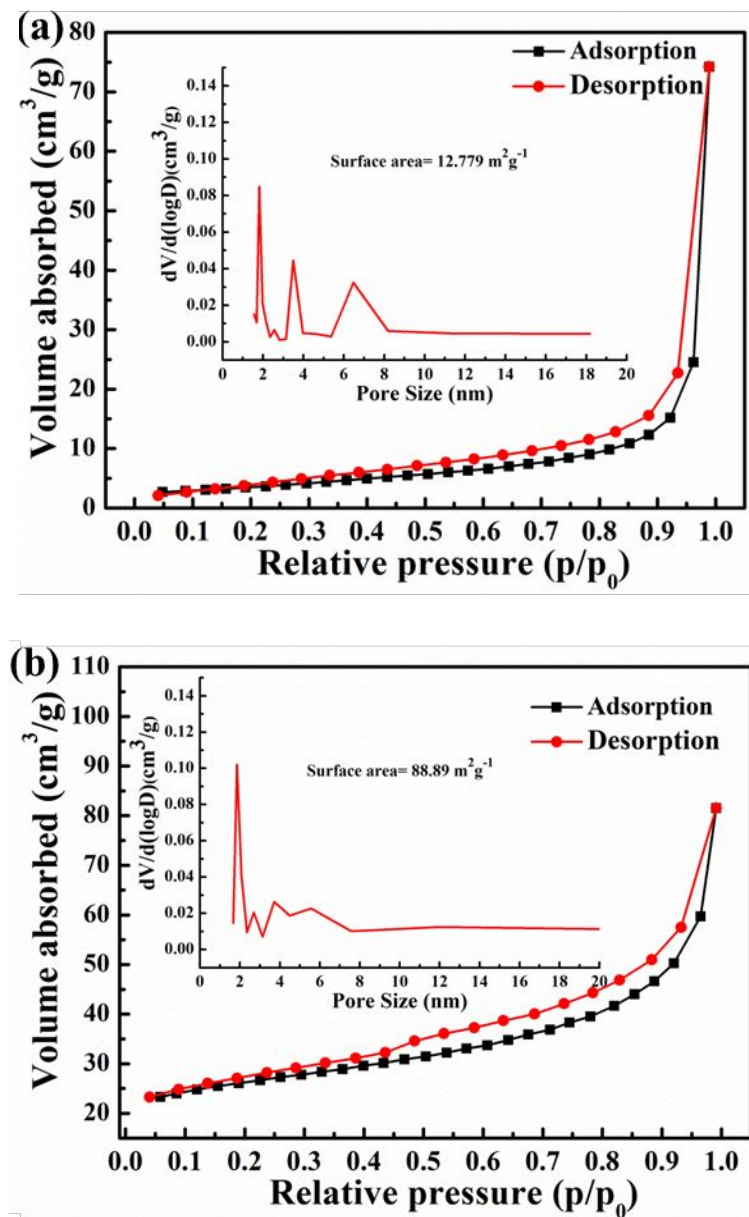


Figure S7 Nitrogen absorption/desorption curves of the NiFe@Zn₃V₃O₈ (a) and NiFe@V₂O₃ (b). Insets are the BJH pore size distribution curves.

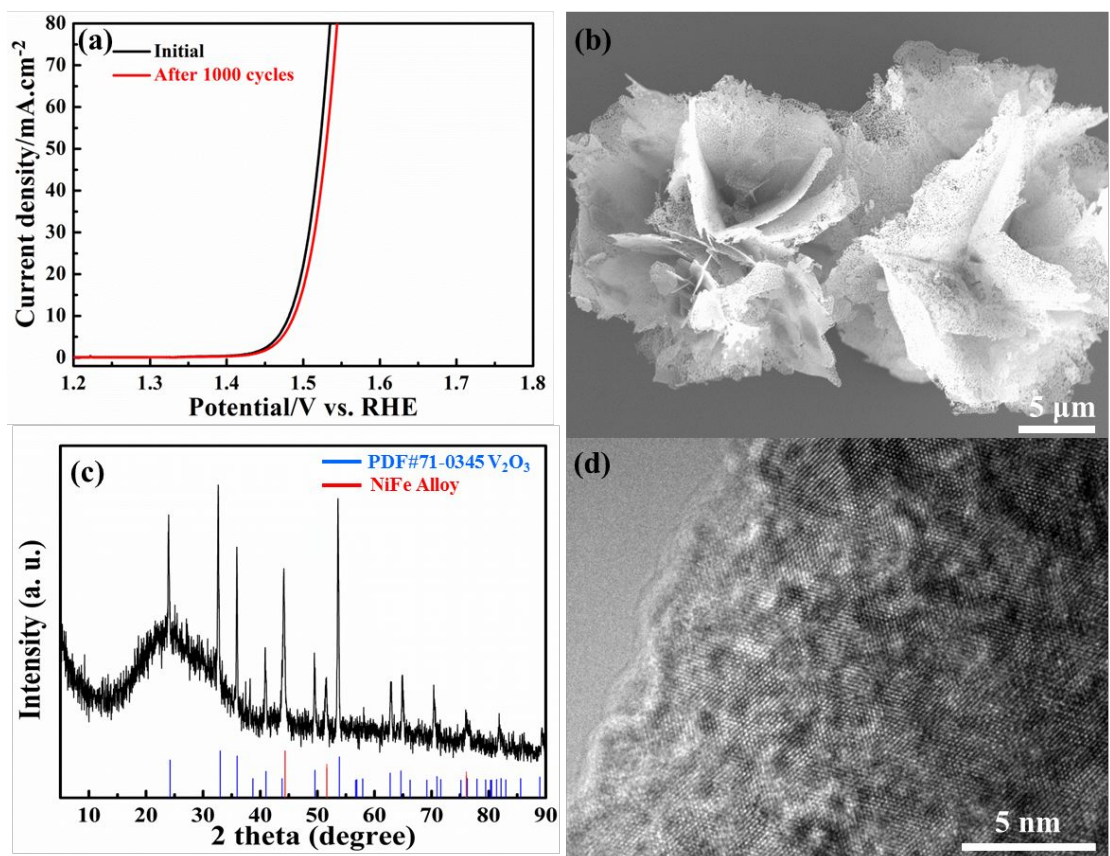


Figure S8 LSV curves of the NiFe@V₂O₃ in 1M KOH after 1000 cycles (a); SEM image (b), XRD pattern (c), and HRTEM image (d) of NiFe@V₂O₃ after long-term test in 1.0 M KOH.

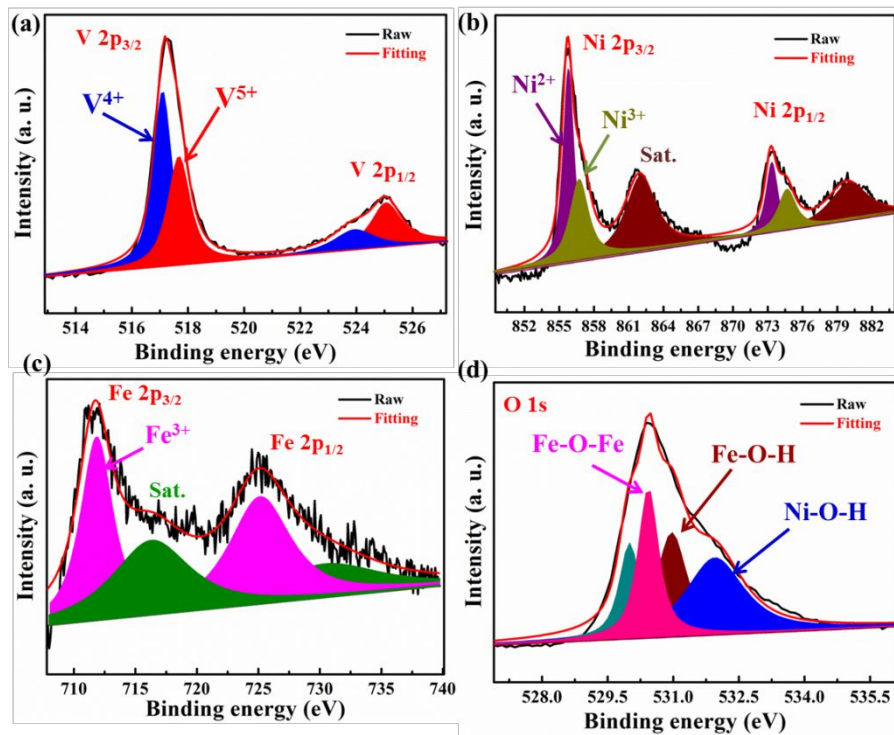


Figure S9 (a) High-resolution XPS spectra of (a) V 2p, (b) Ni 2p, (c) Fe 2p, and (d) O 1s for the NiFe@V₂O₃ hybrid after long-term durability test in alkaline medium.

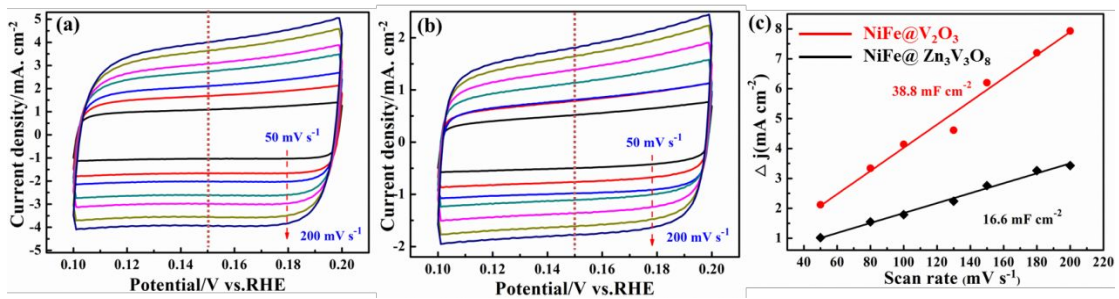


Figure S10 Typical cyclic voltammetry curves of NiFe@V₂O₃ (a), and NiFe@Zn₃V₃O₈ (b) with different scan rates; (c) capacitive current based on scan rate of NiFe@V₂O₃, and NiFe@Zn₃V₃O₈ at the overpotential of 0.15V.

Table S1 Comparison of the electrocatalytic performance of the NiFe@V₂O₃ to other recently reported high performance OER catalysts.

Electrocatalyst	Electrolyte	Tafel slope (mV dec ⁻¹)	η (mV) at 10 mA cm ⁻²	Reference
NiFe@V ₂ O ₃	1 M KOH	51	255	This work
NiFe–MoO _x NS	1 M KOH	55	370	1
FeCoNi alloy	1 M KOH	55	325	2
NiFe/C Hybrids	1 M KOH	54	330	3
Ni ₃ Se ₂ /CF	1 M KOH	80	295	4
NiCo binary oxide	1 M KOH	39	325	5
Co-P	1 M KOH	65	300	6
P,S-CNS	0.1 M KOH	64	330	7
EG/CoSe-NiFe-LDH	1 M KOH	57	250	8

Table S2 Comparison of the electrocatalytic performance of the NiFe@V₂O₃ to other recently reported high performance HER catalysts.

Electrocatalyst	Electrolyte	Tafel slope (mV dec ⁻¹)	η (mV) at -10 mA cm ⁻²	Reference
NiFe@V ₂ O ₃	1 M KOH	85.4	84	This work
FeCoNi alloy	1 M KOH	77	211	²
NiFe/C Hybrids	1 M KOH	111	219	³
Ni ₃ Fe/N-C sheets	1 M KOH	98	72	⁹
NiSe ₂ NCs	1 M KOH	139	540	¹⁰
Co(S _{0.71} Se _{0.29}) ₂	1 M KOH	86	122	¹¹
CoP/CC	1 M KOH	209	129	¹²
Co _{0.5} Mn _{1.5} CH	1 M KOH	/	180	¹³
NiSe/NF	1 M KOH	120	96	⁴

References

- (1) Xie, C.; Wang, Y.; Hu, K.; Tao, L.; Huang, X.; Huo, J.; Wang, S. In situ confined synthesis of molybdenum oxide decorated nickel–iron alloy nanosheets from MoO_4^{2-} intercalated layered double hydroxides for the oxygen evolution reaction. *J. Mater. Chem. A.* **2017**, *5*, 87-91.
- (2) Yang, Y.; Lin, Z.; Gao, S.; Su, J.; Lun, Z.; Xia, G.; Chen, J.; Zhang, R.; Chen, Q. Tuning Electronic Structures of Nonprecious Ternary Alloys Encapsulated in Graphene Layers for Optimizing Overall Water Splitting Activity. *ACS Catal.* **2017**, *7*, 469-479.
- (3) Zhang, X.; Xu, H.; Li, X.; Li, Y.; Yang, T.; Liang, Y. Facile Synthesis of Nickel–Iron/Nanocarbon Hybrids as Advanced Electrocatalysts for Efficient Water Splitting. *ACS Catal.* **2016**, *6*, 580-588.
- (4) Shi, J.; Hu, J.; Luo, Y.; Sun, X.; Asiri, A. M. Ni_3Se_2 film as a non-precious metal bifunctional electrocatalyst for efficient water splitting. *Catalysis Science & Technology* **2015**, *5*, 4954-4958.
- (5) Yang, Y.; Fei, H.; Ruan, G.; Xiang, C.; Tour, J. M. Efficient Electrocatalytic Oxygen Evolution on Amorphous Nickel–Cobalt Binary Oxide Nanoporous Layers. *ACS Nano* **2014**, *8*, 9518-9523.
- (6) Yang, Y.; Fei, H.; Ruan, G.; Tour, J. M. Porous Cobalt-Based Thin Film as a Bifunctional Catalyst for Hydrogen Generation and Oxygen Generation. *Adv. Mater.* **2015**, *27*, 3175-3180.
- (7) Shinde, S. S.; Lee, C.-H.; Sami, A.; Kim, D.-H.; Lee, S.-U.; Lee, J.-H. Scalable 3-D Carbon Nitride Sponge as an Efficient Metal-Free Bifunctional Oxygen Electrocatalyst for Rechargeable Zn–Air Batteries. *ACS Nano* **2017**, *11*, 347-357.
- (8) Tan, Y.; Wang, H.; Liu, P.; Shen, Y.; Cheng, C.; Hirata, A.; Fujita, T.; Tang, Z.; Chen, M. Versatile nanoporous bimetallic phosphides towards electrochemical water splitting. *Energy & Environmental Science* **2016**, *9*, 2257-2261.
- (9) Li, T.; Luo, G.; Liu, K.; Li, X.; Sun, D.; Xu, L.; Li, Y.; Tang, Y. Encapsulation of Ni₃Fe Nanoparticles in N-Doped Carbon Nanotube–Grafted Carbon Nanofibers as High-Efficiency Hydrogen Evolution Electrocatalysts. *Adv. Funct. Mater.* **2018**, *28*, 1805828-1805836.
- (10) Kwak, I. H.; Im, H. S.; Jang, D. M.; Kim, Y. W.; Park, K.; Lim, Y. R.; Cha, E. H.; Park, J. CoSe₂ and NiSe₂ Nanocrystals as Superior Bifunctional Catalysts for Electrochemical and Photoelectrochemical Water Splitting. *ACS Appl. Mater. Interfaces* **2016**, *8*, 5327-5334.
- (11) Fang, L.; Li, W.; Guan, Y.; Feng, Y.; Zhang, H.; Wang, S.; Wang, Y. Tuning Unique Peapod-Like Co(S_xSe_{1-x})₂ Nanoparticles for Efficient Overall Water Splitting. *Adv. Funct. Mater.* **2017**, *27*, 1701008-1701016.
- (12) Tian, J.; Liu, Q.; Asiri, A. M.; Sun, X. Self-Supported Nanoporous Cobalt Phosphide Nanowire Arrays: An Efficient 3D Hydrogen-Evolving Cathode over the Wide Range of pH 0–14. *J. Am. Chem. Soc.* **2014**, *136*, 7587-7590.
- (13) Tang, T.; Jiang, W.-J.; Niu, S.; Liu, N.; Luo, H.; Chen, Y.-Y.; Jin, S.-F.; Gao, F.; Wan, L.-J.; Hu, J.-S. Electronic and Morphological Dual Modulation of Cobalt Carbonate Hydroxides by Mn Doping toward Highly Efficient and Stable Bifunctional Electrocatalysts for Overall Water Splitting. *J. Am. Chem. Soc.* **2017**, *139*, 8320-8328.